Research Article

Di Sheng Lai, Azlin Fazlina Osman*, Sinar Arzuria Adnan, Ismail Ibrahim, Andrei Victor Sandu, Shayfull Zamree Abd Rahim, and Petrica Vizureanu*

The role of natural hybrid nanobentonite/nanocellulose in enhancing the water resistance properties of the biodegradable thermoplastic starch

https://doi.org/10.1515/epoly-2023-0014
received February 22, 2023; accepted May 14, 2023

Abstract: This study focuses on investigating the effect of hybrid nanofillers on the hydration characteristics and soil biodegradability of the thermoplastic corn starch (TPCS) hybrid nanofiller biocomposite (TPCS-HB) films. The data were benchmarked with that of the pure TPCS and TPCS single nanofiller biocomposite (TPCS-SB) as control films. The water absorption properties of TPCS, TPCS-SB, and TPCS-HB films were analyzed and fitted with the standard Guggenheim–Anderson–de Boer equation to study the water activity of the films. Besides, the water permeability test, water vapor permeability, and soil biodegradability of the films were also studied and correlated with the films' surface morphology. The results indicated that the TPCS-HB films possess excellent hydration resistance and comparable biodegradable rate with the TPCS-SB films. The optimal water resistance properties were achieved when the optimal ratio of nanobentonite/nanocellulose (4:1) was incorporated into the TPCS matrix. The outcomes of this study provide an innovative idea and new insights that, by using natural and hybrid nanofillers, the hydrophobicity of the TPCS films could be enhanced. TPCS-HB films show great potential to be developed into a fully green biodegradable TPCS biocomposite film, especially for single-use plastic applications.

Keywords: thermoplastic starch, nanocellulose, bentonite, bioplastic, environmentally friendly.

1 Introduction

Thermoplastic starch (TPS) is one of the most promising bio-based polymers to replace petrochemical-based plastics, especially for single-use packaging applications (1).

*** Corresponding author: Azlin Fazlina Osman,** Faculty of Chemical Engineering Technology, Universiti Malaysia Perlis (UniMAP), Arau 02600, Perlis, Malaysia; Biomedical and Nanotechnology Research Group, Center of Excellent Geopolymer and Green Technology (CEGeoTech), Universiti Malaysia Perlis (UniMAP), Arau 02600, Perlis, Malaysia, e-mail: azlin@unimap.edu.my
*** Corresponding author: Petrica Vizureanu,** Gheorghe Asachi Technical University of Iasi, Faculty of Materials Science and Engineering, Blvd. D. Mangeron 71, 700050, Iasi, Romania; Technical Sciences Academy of Romania, Dacia Blvd 26, 030167 Bucharest, Romania, e-mail: peviz@tuiasi.ro
Di Sheng Lai: Faculty of Chemical Engineering Technology, Universiti Malaysia Perlis (UniMAP), Arau 02600, Perlis, Malaysia; Biomedical and Nanotechnology Research Group, Center of Excellent Geopolymer and Green Technology (CEGeoTech), Universiti Malaysia Perlis (UniMAP), Arau 02600, Perlis, Malaysia, e-mail: disheng.lds@gmail.com
Sinar Arzuria Adnan: Faculty of Chemical Engineering Technology, Universiti Malaysia Perlis (UniMAP), Arau 02600, Perlis, Malaysia; Biomedical and Nanotechnology Research Group, Center of Excellent Geopolymer and Green Technology (CEGeoTech), Universiti Malaysia Perlis (UniMAP), Arau 02600, Perlis, Malaysia, e-mail: sinar@unimap.edu.my
Ismail Ibrahim: Faculty of Chemical Engineering Technology, Universiti Malaysia Perlis (UniMAP), Arau 02600, Perlis, Malaysia; Biomedical and Nanotechnology Research Group, Center of Excellent Geopolymer and Green Technology (CEGeoTech), Universiti Malaysia Perlis (UniMAP), Arau 02600, Perlis, Malaysia, e-mail: ismailibrahim@unimap.edu.my
Andrei Victor Sandu: Gheorghe Asachi Technical University of Iasi, Faculty of Materials Science and Engineering, Blvd. D. Mangeron 71, 700050, Iasi, Romania; Romanian Inventors Forum, Str. Sf. P. Movila 3, 700089 Iasi, Romania; National Institute for Research and Development in Environmental Protection INCDPM, Splaiul Independentei 294, 060031 Bucuresti, Romania, e-mail: sav@tuiasi.ro
Shayfull Zamree Abd Rahim: Faculty of Mechanical Engineering & Technology, Universiti Malaysia Perlis (UniMAP), Arau 02600, Perlis, Malaysia

TPS, a biodegradable, low-cost, and renewable plastic, which has the same processing properties as petrochemical-based plastics, has attracted a lot of attention from researchers to further improve the mechanical properties of TPS (2–4). Granule starch comprises two polysaccharide macromolecules, amylose (linear chain) and amylopectin (highly branched chain), which interact with very strong intra- and inter-hydrogen bonding, resulting in several double helix microcrystalline structures. Due to the mega intra- and inter-hydrogen bonding between the polymer chains, starch granules experience decomposition instead of melting during processing in the heat. Thus, incorporating a plasticizer such as a polyol, water, formaldehyde, and urea is required to form TPS films with good durability. TPS films can be produced via several plastic film processing methods such as casting, blowing, and extrusion.

Generally, TPS films exhibit excellent filmogenic property with high gas barrier properties and non-toxicity, which is highly suitable for food packaging applications. However, the TPS films have some limitations, such as low mechanical strength and hygroscopicity, compared to other commodity resins (5). Besides, the high retrogradation rate of TPS films also limits the stability of TPS films during their service life and makes them less competitive compared to conventional plastic films. The high hygroscopicity of the pure TPS films always promotes high water absorption in the films and leads to a high retrogradation rate in TPS films, which causes detrimental effects to the TPS films (6). Several strategies and modifications were applied to enhance the hydration resistance properties and mechanical properties of starch-based films, such as by blending with petrochemical-based or other bio-based plastics (7), crosslinking and chemical modifications of the starch chain structures (8), incorporating different plasticizers (9), and developing nanocomposite films (10,11).

Numerous studies were carried out profoundly to study the toxicity of nanoclay and nanocellulose toward human cells, proving each filler was non-toxic to human cells and safe to be consumed (12,13). The studies also showed that most of the toxicity of the nanofiller was often associated with the chemical modifier of the nanofiller (13). Due to food contact safety and biodegradable properties of the films, the chemical modification of starch granules or blending with another petrochemical polymer was highly discouraged and lambasted by environmentalists (14,15). Therefore, natural fillers such as clay and nanocellulose, which were non-toxic and highly compatible with TPS, were investigated extensively by researchers to enhance the mechanical properties and hydration properties of the TPS films. Apart from enhancing the mechanical properties of the TPS films, nanoclay, and nanocellulose also improved the TPS films' water resistance properties.

The excellent dispersion (exfoliation or intercalation) of the nanoclay silicate structure in the TPS films provided a tortuous path in the TPS films, which inhibited the diffusion of water molecules and increased the water resistance properties (16). Besides, nanocellulose, which has a similar chemical structure to the TPS chain, was also reported to enhance the TPS hydration properties due to the high crystallinity and was able to form nanocellulose percolation structure in the TPS matrix (17). However, several studies reported a contradictory conclusion that incorporating nanoclay and nanocellulose in the TPS films has a less adverse effect on the TPS films' water resistance properties (2,18,19). Based on their studies, the lower effect of nanoclay and nanocellulose on the water resistance properties was due to the poor dispersion of nanofillers in the TPS, as high contact surface nano-sized filler was more preferably agglomerated. The highly agglomerated nanofiller reduces the interaction between the TPS and nanofiller, resulting in microvoid formation in the TPS matrix and promoting the accumulation of water molecules in TPS films.

Several reports verified that incorporating nanocellulose in TPS can enhance the diffusion of water molecules through the TPS matrix due to its high affinity toward water molecules (19,20). From the literature, we can conclude that enhancing the water resistance properties of the TPS films by incorporating a single filler was inconsistent and highly dependent on nanofiller dispersion. The inconsistent hydration properties of the TPS/nanocellulose films and tedious controllable dispersion of the nanofiller have increased the challenges for the production of TPS films on a large factory scale and in industrialization.

Concerning the above matter, chemical modification through esterification, acylation, crosslinking, or silylation can be applied to reduce the inconsistency of hydration characteristics of the nanocellulose by introducing hydrophobic structures into the nanocellulose structures for increasing the water resistance properties (21–23). However, the chemical modification of nanocellulose again raises the food toxicity concern, which limited the TPS/nanocellulose films' application, especially in food packaging (23). Therefore, the idea of hybridization of nanocellulose with nanoclay was developed to overcome the inconsistency in the hydration properties of the TPS/nanocellulose films. The high aspect ratio and platelet-sized nanoclays are well-described in numerous studies to effectively reduce the water permeability and the water sensitivity of the TPS films by providing more

complex and tortuous pathways for the diffusion of water molecules (24–27). Besides, the hybridization of nanocellulose with nanoclay was reported to be effective in enhancing the gas barrier properties of films. Wu et al. reported that the gas barrier properties of the nanocellulose/montmorillonite composite films improved five times compared to the nanocellulose films without nanoclay (28). Garusinghe et al. developed nanocellulose composite films with high barrier properties by varying the montmorillonite content. They showed that the good distribution of nanoclay in the nanocellulose composite could not only enhance the barrier properties of the films but also the mechanical properties of the biocomposite films (29). The use of hybrid nanofillers not only retained the intrinsic advantages of the nanocellulose but further enhanced the composite barrier properties through the synergic effects of the hybrid nanofillers.

As reported in our previous studies, hybrid nanofiller, nanobentonite, and nanocellulose were proven to effectively enhance the mechanical properties (30) and low retrogradation rate of TPS films (31) due to the synergy effect of hybrid nanofillers with the TPS chain than a single nanofiller. To the best of our knowledge, no literature or study reported the hydration and biodegradable properties of TPS/nanobentonite/nanocellulose biocomposite films, which is one of the most crucial properties of TPS films in film packaging applications. In this study, the effect of nanobentonite and nanocellulose on the hydration and biodegradable properties of the TPS films was investigated further to complete the comprehensive study of the TPS hybrid biocomposite films. The main goal of this study is to enhance the hydration properties of thermoplastic corn starch (TPCS) films with the natural hybrid nanofiller.

Incorporating hybrid nanobentonite and nanocellulose represents a novel, low-cost, and simple method to significantly enhance the hydration properties of TPCS films without sacrificing the biodegradable properties. The water absorption and diffusion of all the TPCS films were studied by moisture absorption and water permeability tests. Meanwhile, the films' surface hydrophilicity and the water stability were determined by measuring the water contact angle (WCA) formed on the films and the water-soluble test. Furthermore, the films' morphology, which is associated with the films' surface hydrophilicity properties, was observed using a scanning electron microscope (SEM). Finally, the biodegradation rate and the physical erosion of all TPCS biocomposite films were investigated by the soil biodegradability analysis for 3 months.

2 Materials and methods

2.1 Materials

Corn starch with a granular size of 2–30 μm (72% amylopectin, 28% amylose) was purchased from Sigma Aldrich (St. Louis, MO, USA). It was plasticized into a thermoplastic film called TPCS. The nanocellulose (average width, 3–5 nm; average length, <150 nm) and nanobentonite powder (average particle size, ≤25 μm; Nanoclay, Nanomer PGV) were incorporated to form the hybrid nanofillers (N + B) of the TPCS hybrid biocomposite films. The nanocellulose was extracted from the oil palm empty fruit bunch fiber purchased from United Oil Palm Industries Sdn Bhd (Nibong Tebal, Malaysia). Natural nanobentonite clay was obtained from Sigma-Aldrich (St. Louis, MO, USA). The detailed preparation method of the hybrid nanofiller was reported in our previous study (30). Glycerol, which was purchased from HmbG Chemicals (Hamburg, Germany), and distilled water were used as plasticizers in the formation of TPCS films.

2.2 Preparation of TPCS, TPCS-SB, and TPCS-HB films

Three types of films, the original TPCS, the TPCS single nanofiller biocomposite (TPCS-SB) films, and the TPCS hybrid nanofiller biocomposite (TPCS-HB) were casted. For the pure TPCS films, 5 g of corn starch was combined with 100 mL of distilled water and 2 g of glycerol. A heated magnetic stirrer was used to agitate the mixture at 300 rpm for 30 min at 80°C to create a homogeneous TPCS gel. To produce TPCS-SB and TPCS-HB films, 5% of a single nanofiller or hybrid nanofillers with different ratios of nanocellulose/nanobentonite were mixed with 20 mL of distilled water and processed with ultrasonic technology to promote the high dispersion of the nanofiller. The nanofiller solvent was then combined with the TPCS gel and stirred continuously for 15 min. For the TPCS-HB films, two hybrid nanofiller ratios were selected: 4B:1C and 2B:3C. These two ratios were selected because, as shown in our previous study, 4B:1C was found to be the optimum ratio to produce the toughest films, while 2B:3C was observed to result in the TPCS-HB film with the lowest toughness value.

After completion of stirring the mixture, it was poured into an 8 in. Teflon casting mold and dried in the oven at 45°C for 24 h. The composition and the abbreviation of the samples are presented in Table 1.

Table 1: Formulation of TPCS, TPCS-SB, and TPCS-HB films

	Acronym	Starch (wt%)	Bentonite (wt%)	Nanocellulose (wt%)
Pure TPCS	TPCS	100	0	0
TPCS-SB	TPCS/5B	95	5	0
	TPCS/5C	95	0	5
TPCS-HB	TPCS/4B1C	95	4	1
	TPCS/2B3C	95	2	3

2.3 Testing and characterization of films

2.3.1 Moisture absorption test

The moisture absorption test was carried out according to ASTM D5229 to determine the rate of absorption of film samples. The selected films were cut into 4.0 cm × 4.0 cm and dried in the oven at 50°C for 24 h to completely remove the water content in the films. The films were weighted initially to record the initial weight before starting the absorption moisture test. For regular periods, the film samples' weights were recorded to determine the rate of absorption. The moisture absorption test was repeated five times for each sample formulation, and average values were recorded. The moisture absorption of films is calculated as shown in Eq. 1:

$$\text{Moisture absorption}(\%) = \frac{(W_a - W_o)}{W_o} \times 100\% \quad (1)$$

where W_a is the weight of humid films after absorption of moisture and W_o is the initial weight of films after drying in an oven for 24 h.

The water sorption analysis of the films at different humidities was carried out inside a desiccator with salt water (LiCl, $MgCl_2$, K_2CO_3, Mg $(NO_3)_2$, $NaNO_2$, NaCl, and KCl) to maintain the relative humidities (RHs) of 23%, 33%, 43%, 53%, 64%, 73%, 80%, and 100% at 25°C. The Guggenheim–Anderson–de Boer (GAB) equations were used to model the water sorption experimental data. The modeling of the moisture content of the films was done by using origin software. The GAB equation is as follows:

$$X_w = \frac{Ckm_o a_w}{[(1 - Ka_w + CKa_w)]} \quad (2)$$

where X_w is the steady state moisture content, a_w is the water activity, m_o is the monolayer water content, and C and k are constant values depending on the temperature by the Arrhenius-type equation, which represent sorption heat of the first and multilayer, respectively.

Eq. 2 is written in another form (Eq. 3), which is used for the calculation of the parameters m_o, K, and C. A more detailed derivation of Eq. 3 can be obtained from the study of Blahovec and Yanniotis (32):

$$\frac{a_w}{X_w} = \frac{K(1 - C)}{m_o C} a_w^2 + \frac{C - 2}{m_o} a_w + \frac{1}{Km_o C} \quad (3)$$

2.3.2 Water solubility test

The water solubility test of the films was performed by using samples of 5 cm × 5 cm × 0.2 mm dimension immersed in the deionized water. Before immersing in the deionized water, all the films were dried in the oven at 50°C for 12 h to remove the adsorbed water content. All the dried films were fully immersed at least 5 cm underneath the deionized water at 25°C for 24 h. The film samples were dried in an oven for 12 h at 50°C to completely remove the moisture in the films. For each film's formulation, five duplicates were tested, and the average value was calculated for data integrity. The water solubility of the films was calculated by using the following equation:

$$\text{Moisture content}(\%) = \frac{W - W_o}{W} \times 100\% \quad (4)$$

where w is the weight of films after drying in the oven before immersing in deionized water and w_o is the weight of films after drying in the oven after immersing in deionized water. The test was repeated three times to obtain the average value of the moisture content.

2.3.3 WCA

The WCA was measured based on the sessile drop technique, according to Boinovich and Emelyanenk (33). The apparatus consisted of a mobile base with a sample holder, a high-resolution digital camera, and a light source. A 4.0 mm × 4.0 mm film sample was glued on the sample's holder to obtain a flat and even film surface. About 5 µL of distilled water was dropped on the air-facing side of the samples at 25°C, and the water droplet was measured after 10 s for stabilization. This amount of water was employed because it could minimize the water gravitation flattening effect. The test was repeated five times, and the average value was obtained and recorded. A 20 cm distance between the digital camera lens and the film sample was set up to obtain a sharp and good image. The angle calculation methodology was based on the shape of the distilled water droplet image formed by

the intersection of the liquid and solid. The software used to calculate the contact angle was Image-J powered and licensed by BSD-2.

2.3.4 Water vapor permeability (WVP)

The WVP of the films was determined by using ASTM E 96 for the cup method where the WVP of films was calculated when the water vapor transmits out from the container under constant temperature and humidity. TPCS, TPCS-HB, and TPCS-SB films were prepared in even thickness (0.20 mm). A constant amount of distilled water was filled into the container (19 mm depth) and TPCS films were attached and sealed with rubber to the container to prevent the leakage of water around the container edges during the testing. The testing temperature and humidity were regulated within 1°C and 2%, respectively. Constant airflow conditions were required to maintain good circulation of air in the test location. The container with TPCS films was weighed and the reading was recorded as the initial weight. The weight of specimen is weighed periodically (6 h) until the rate of change remains substantially constant. The water permeability test was repeated four times for each film's formulation. The rate of water vapor transmission was calculated using the following formula:

$$\mathrm{WVT} = \frac{G}{tA} = S \times A \tag{5}$$

where WVT is the rate of water vapor transmission ($g{\cdot}h^{-1}{\cdot}m^{-2}$), G is the weight loss (straight line of the curve; g), S is the slope of the straight line ($g{\cdot}h^{-1}$), A is the area of the cup mouth (test area; m^2), and t is the time interval (h). The rate of WVP is calculated as follows:

$$\mathrm{WVP} = \frac{\mathrm{WVT}}{\Delta p} = \frac{\mathrm{WVT}}{\mathrm{S}(R1 - R2)} \tag{6}$$

where Δp is the vapor pressure difference (mmHg), S is the saturation vapor pressure at the test temperature, $R1$ is the RH in the container in fraction, and $R2$ is the RH of the environment in fraction.

2.3.5 SEM

The film's surface structure and morphology were observed using an SEM (JEOL JSM-6460LA; JEOL Ltd, Japan). The surface morphology of all the films was observed under an SEM and compared. Before capturing the images, the film's surface was coated with platinum using a JFC-1600 Auto Fine Coater (JEOL Ltd, Japan) for obtaining the optimal SEM image.

2.3.6 Biodegradability test (soil burial test)

The soil burial test was carried out according to EN ISO 846: 1997. The test soil with 60% moisture content was filled into a 1 L plastic container. The film samples were cut into 6.0 cm × 3.0 cm size and buried in the soil at a depth of 5 cm for a duration of 3 months. The soil was sprayed with 10 mL of distilled water weekly to maintain the same soil moisture content for 3 months. Five film samples were tested for each film's formulation. Each sample was taken out and the soil attaching to the surface of the films was removed at constant time intervals. The degradation rate was calculated by the weight loss rate of films at regular times. The films were dried in an oven for 24 h at 50°C and then weighed before burying in the soil. The weight loss of films is calculated using the following equation:

$$\text{weight loss}(\%) = \frac{W_\mathrm{i} - W_\mathrm{d}}{W_\mathrm{i}} \times 100 \tag{7}$$

where W_i is the initial weight of dry samples and W_d is the weight of the sample recovered from the soil.

3 Results and discussion

3.1 Water absorption of TPCS, TPCS-SB, and TPCS-HB

Generally, it is understood that the water content of all the biopolymeric films increases with the increase in RH, while the water absorption of films will finally reach an equilibrium water content percentage (1,4). In this study, water absorption and water solubility analysis were performed on the pure TPCS, TPCS-SB, and TPCS-HB films. Based on the results summarized in Table 2, the pure TPCS film indicates the highest moisture adsorption, while TPCS/4B1C possesses the lowest water adsorption at all humidity values. All the TPCS-SB films have lower moisture adsorption when compared to those of the pure TPCS film, showing that incorporating nanofiller (nanobentonite or nanocellulose) could alter the surface morphology and the active water molecules were adsorbed on the film's surface. As expected, the TPCS-HB films showed lower moisture absorption rates compared to

Table 2: Water solubility, WVP, and GAB parameters from isotherms of TPCS, TPCS-SB, and TPCS-HB films; the coefficient of determination ($R2$) > 0.96 for all fitted models

	GAB parameters					
Films' formulation	M_o	K	C	$R2$	**Water solubility (%)**	**WVP × 10^{-12} (g·m^{-1}·s^{-1}·Pa^{-1})**
TPCS	12.350	0.772	3.186	0.992	33.45	3.56
TPCS/5B	10.040	0.550	5.005	0.977	27.73	2.53
TPCS/5C	9.970	0.689	5.417	0.979	26.98	2.84
TPCS/4B1C	7.770	0.504	6.345	0.960	21.76	2.03
TPCS/2B3C	8.910	0.547	4.313	0.964	23.93	2.23

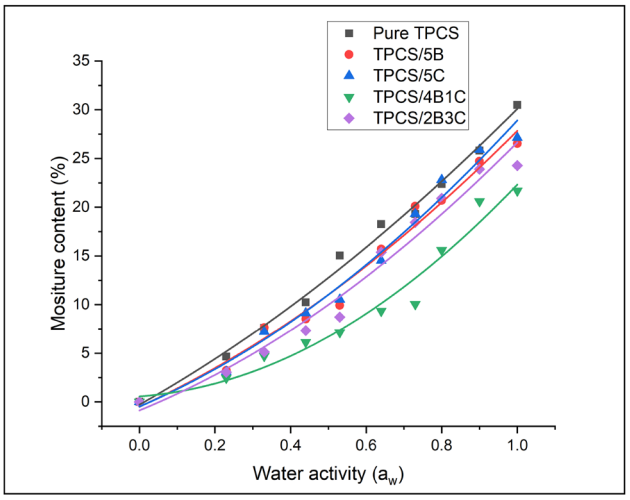

Figure 1: Experimental and calculated GAB water isotherms of TPCS, TPCS-SB, and TPCS-HB films.

those of the TPCS-SB films. The better resistance toward moisture absorption by the hybrid biocomposite system shows that the synergic effect of the hybrid nanofiller helps to improve the films' toughness and water absorption. The experimental data for the moisture adsorption content of the films fitted with GAB equations are shown Figure 1. The moisture sorption GAB parameter showed $0 < K \leq 1$ and $C \geq 2$, indicating a type II as modeled with GAB equations.

Each parameter in the GAB equation represents a physical meaning where C is the enthalpic differences of sorption for the monolayer to the primary binding sites. The higher the C, the stronger the water binding to the primary layer. Meanwhile, K is defined as the enthalpic difference of sorption for bulk water with the multilayer water layer structure on the films. The higher the value of K, the higher the water molecules' mobility in bulk molecules and fewer distinction properties between the multilayer water molecules and the bulk water molecules. M_o denotes the moisture content corresponding to the "monomolecular layer" on the whole free surface of a material. Meanwhile, according to the literature, the sigmoidal shape of the isothermal graph can be divided into three regions: $a_w < 0.2$, $0.2 < a_w < 0.6$, and $a_w > 0.6$, where each region represents the monolayer adsorption of water molecules (physio-sorbed to the surface), multilayer adsorption of water molecules on the polar size, and the progressive water molecules absorbed at subsequent layers, respectively (34).

For a more decisive conclusion, surface morphology and the pores formed on the TPCS films were observed using SEM and are shown in Figure 2. It is evident that the porosity of the films will affect the water absorption in the films. Kulasinski et al. showed that the porosity on the biopolymer surface is in a linear relationship with the water adsorption content, where the porosity could act as the space for the accumulation of water molecules (35). They found that the accumulated water in the pores could further push the polymer chains by breaking up the interchain hydrogen bonding between biopolymers, creating more significant porosity and enabling higher adsorption. The pure TPCS films exhibited a firm granular structure with big pores and voids throughout the surface of the films, as shown in Figure 2. The number and the size of the pores decreased after a single filler was incorporated into the matrix. The compatibility and the compressibility of TPCS/5B and TPCS/5C were higher than those of the pure TPCS matrix, as observed in the SEM image. Meanwhile, as the 4B1C hybrid nanofillers were incorporated into the TPCS matrix, the porosity of the films was almost removed. This feature can be observed in the image of the TPCS/4B1C film (Figure 2d). The degree of films' porosity was arranged in the order TPCS > TPCS/5B > TPCS/5C > TPCS/2B3C > TPCS/4B1C.

It was found that the sequence order of M_o is in line with the degree of the films' porosity, as shown in Figure 2, where the higher the porosity, the higher the M_o. The higher M_o indicated that the number of water molecules to form a monolayer on the whole surface of the films

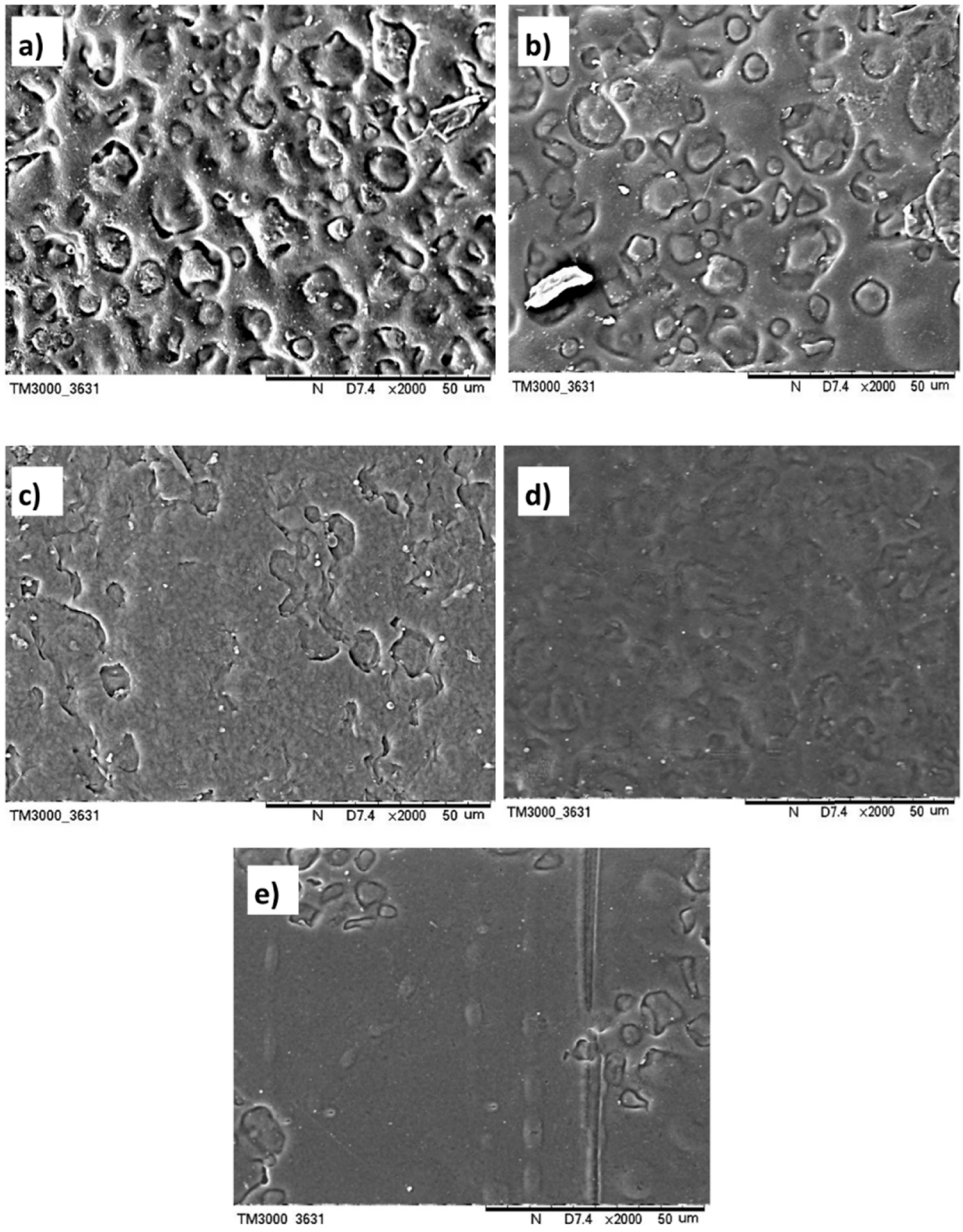

Figure 2: Surface morphology of (a) pure TPCS, (b) TPCS/5B, (c) TPCS/5C, (d) TPCS/4B1C, and (e) TPCS/2B3C, as observed under 2,000× magnification.

increased with increased porosity. The increase of water molecules to form the monolayer was due to the ink bottle phenomenon where the pores formed on the films followed the characteristics of an ink bottle (36). The monolayer water molecules were adsorbed into the wall and the neck of the pores until the water molecules filled up the pores, which may act like a closed pore. Therefore, more water molecules were required to bridge the water molecules across the pores to form the monolayer structure across the films. The pure TPCS film possesses the most substantial water-holding power due to the high pores' surface morphology. Meanwhile, the compact morphology of the TPCS/4B1C resulted in the least water-holding power, as the water molecules only can form on the surface area.

Besides, the interaction of monolayer water molecules with the TPCS surface and the way of water molecules are organized in layers can be predicted by combining C and K values. The organization of different water molecules in the monolayer, multilayer, and internally absorbed (bulk) water can be studied by combining C and K values. For the pure TPCS films, it possesses the lowest C and highest K values compared to other films, indicating that

the monolayer water molecules are less firmly bound to the primary sorption sites as the contact surface between water molecules was least due to the highest pore structure in TPCS films. Meanwhile, the highest K values indicate that the water absorbed on the TPCS surface has the highest mobility, which is the same characteristic as the water molecules in the bulk liquid. On the other hand, the TPCS biocomposites with single filler show different trends of water absorption characteristics. Particularly, the TPCS/5C has higher C values compared to the TPCS/5B, indicating that the monolayer water has formed a more vital interaction with the TPCS/5C due to its more compact structure (Figure 2). Meanwhile, the lower C values of the TPCS/5B may also contribute to bentonite's less hydrophilic properties than the nanocellulose, reducing the adsorption of the monolayer water molecules on the films. Furthermore, the TPCS/5C also exhibited a higher K value than the TPCS/5B, showing that the water molecules formed above the monolayer have higher mobility than the TPCS/5B.

On the contrary, the TPCS/4B1C exhibited the lowest K values and the highest C values compared to all the films. The highest C values shown by TPCS/4B1C indicate that the monolayer water molecules have the strongest interaction with the film's absorption side while the lowest K values also show that the water molecules at the subsequent layer are arranged in a layer structure that has less mobility compared to the bulk liquid. The high C values and the low water content of TPCS/4B1C suggest that the wetting of the TPCS/4B1C surface is possible; however, only a thin layer of water molecules was cohered to the surface of the film. The low K values showed that the water layer formed on the monolayer of water molecules was highly oriented, showing that the spreading of water molecules on the films is limited. The strong hydrogen bond interaction between the monolayer water molecules and the TPCS surface, and, within the structure, water molecules reduced the hydrogen bonding sites for more water molecules to adhere to the TPCS surface (5).

Generally, the hydrogen bonding site was confined to the layer structure of water molecules. The structure of confined water molecules resembles a solid ice-like network where the water molecule forms tetrahedrally coordinated in a fixed position, and the mobility of water molecules in this region is restricted. The formation of a high-order structure water molecule layer provides a hydrophobic surface than other films. However, the effect of the structure water molecules deteriorated, observed in the TPCS/2B3C films, as the K values increased, indicating that the structure water molecules were less oriented and had higher mobility. This may be due to the higher porosity density of TPCS/2B3C compared to that of TPCS/4B1C.

Meanwhile, the lower K values for the TPCS/4B1C films also showed the lower water molecules being absorbed into the films due to the high orientation of the water molecule's structure (37). This concept was the same as the ice-water theory, where ice has less density of water molecules than that of bulk water as the water molecules in ice have fixed and oriented water molecules, arranged in the solid structure. The lowest K values of TPCS/4B1C show that the water absorbed on its surface prefers to orientate in a layered pattern, which restricts the water molecules from diffusing into the structure. Meanwhile, the high K values show that the adsorbed water on the film's surface has a less oriented structure and high mobility like bulk water, which can allow a high number of water molecules to diffuse into the structure and increase the water absorption in the film.

3.2 Water solubility of TPCS, TPCS-SB, and TPCS-HB films

The water solubility test was performed to analyze the stability of TPCS, TPCS-SB, and TPCS-HB films. The water solubility test is an important parameter that indicates the product's stability in the aqueous medium and determines the film's application. The pure TPCS film exhibited the highest water solubility; however, the water solubility was significantly reduced when nanofillers were incorporated (Table 2). A further improvement in the water solubility resistance was observed for hybrid nanofiller films as they showed a 5% decrease in the water-soluble content than the TPCS-SB films. The lowest water solubility exhibited by TPCS/4B1C films indicated a closed-pack and a firm nacre structure could withstand the osmosis pressure in the TPCS matrix, restrict the motion of the amorphous region, and maintain the firm 3D network structure of the TPCS matrix. The high crystallinity of nanocellulose and tortuous structure induced by bentonite filler synergistically prevent the TPCS film contents from moving in and out when immersed in the water. Besides, the lower water solubility may be due to the lower availability of the TPCS hydroxyl group and a strong filler TPCS interaction, which hinder the diffusion of water molecules into the TPCS matrix. The water solubility of TPCS films was in the order of TPCS > TPCS/5B > TPCS/5C > TPCS/2B3C > TPCS/4B1C films.

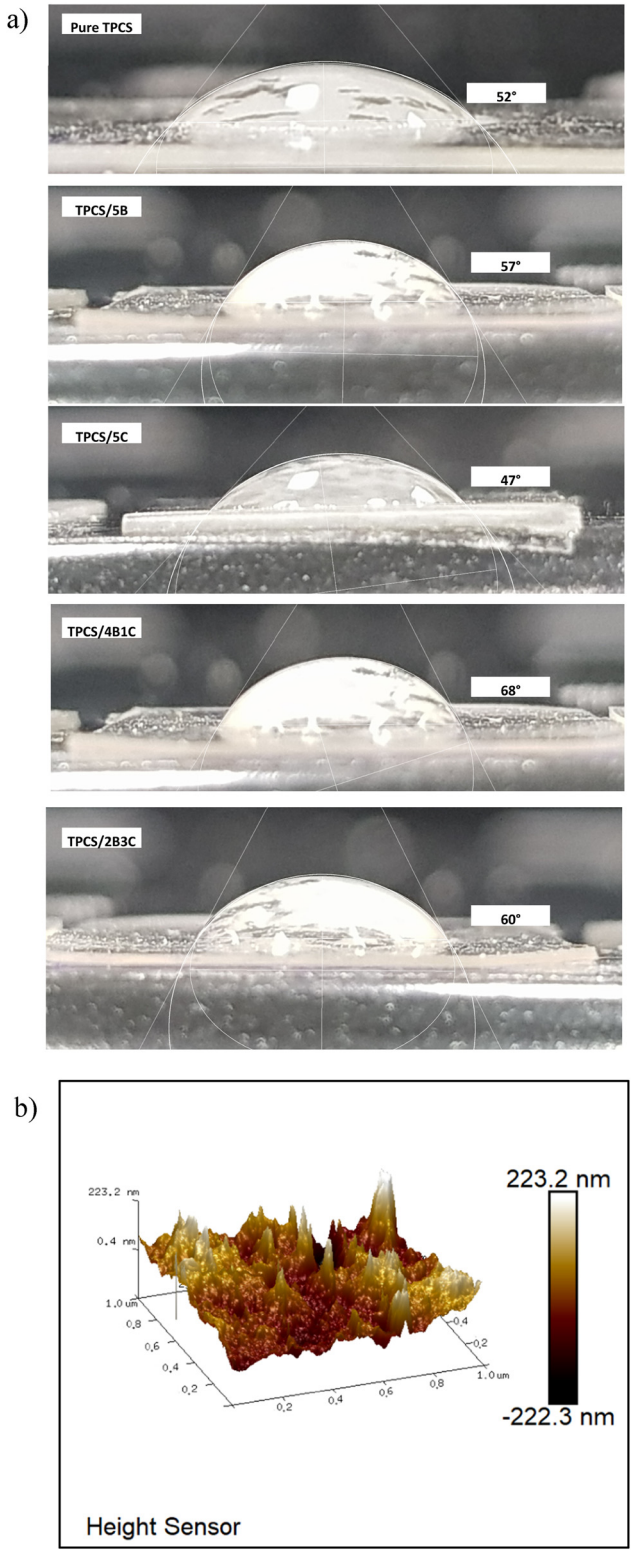

Figure 3: (a) WCA values of TPCS, TPCS-SB, and TPCS-HB films. (b) 3D topology image of TPCS/4B1C films.

3.3 Surface hydrophobicity of TPCS, TPCS-SB, and TPCS-HB films observed through WCA

The surface hydrophobicity can be determined by measuring the WCA formed on the film's surface, as shown in Figure 3. WCA reflected the physicochemical response of the pure solvent on the film's surface. Biopolymer films always have low WCA values due to the solid intermolecular interaction of hydrogen bonding size with the film's surface. Generally, if the film's surface energy is greater than the water surface tension, the water droplet will appear in a flatter shape; on the other hand, the water droplet will appear spherical when the WCA is high. The increase or decrease of WCA is highly dependent on the changes in the surface roughness and the water molecules' mobility and orientation when interacting with the TPCS films. He et al. (38) showed that the micro-/nano-hierarchical architectures on the film's surface have a much higher effect on the wettability of TPCS films than the films' surface energy.

The WCA of the TPCS biocomposite films was higher compared to that of the pure TPCS film, indicating that the hydrophobicity of the film's surface increased as a nanofiller was added to the matrix. The surface contact angle of the untreated TPCS was 52°, which is in line with the result of Yin et al. (39). The lower WCA values of the pure TPCS and TPCS-SB films compared to those of the TPCS-HB films may be attributed to the high pore structure on the film's surface (Figure 2), which destroy and create unbalanced surface tension of the water droplet by adsorbing the water molecules to fill up the pores through capillary forces. The TPCS-SB films have higher WCA values than pure TPCS film as the pore's density is reduced, which shows that the hierarchical architectures in the film surface have a significant impact on the films' hydrophobicity. Besides, the TPCS film surface incorporating nanobentonite or nanocellulose could reduce the active site for hydroxyl group interaction and lower the film's surface energy with water droplets. The reduced surface energy reduces the interaction between water droplets and the film's surface and leads to higher WCA than the pure TPCS films (40).

On the other hand, the TPCS-HB film's surface displayed a highly compact and less porous structure (Figure 2), and thus less degree of interaction between the water droplets and the film surface was established. The high WCA shows that the hybrid nanofillers could significantly improve the

hydrophobicity of the films. This hydrophobic effect was not observed in the TPCS-SB films or the pure TPCS film. As shown in previous studies, hydrophobicity is usually proportional to the surface roughness of the films. Therefore, the TPCS/4B1C films that exhibited the highest WCA could be due to the nano-hierarchical architectures on its film's surface. The nanoscale potholes on the surface of this sample could not be detected by the SEM image; however, they can be verified through surface topological analysis using atomic force microscopy (AFM) (Figure 3b).

The nanostructure surface of the TPCS/4B1C film can result in a high hydrophobic effect, which can be associated with the rose petal effect, as explained in the study of Bushan and Nosonovsky (41). Based on the previous study, the increase of polymer WCA would be attributed to the "lotus leaf" effect, where the high roughness of the film's surface can create a liquid–vapor interface between the water droplet and film surface. The micro-air gap formed between the interaction of water droplets and the film's surface induces high WCA by reducing the interaction of water and the film's surface, just like the lotus leaf (40). However, the high adhesion of water molecules toward the TPCS-based films showed that the lotus leaf effect may not be appropriate to explain the increase of WCA values of the TPCS and TPCS biocomposite films. The high affinity of water molecules toward the TPCS could penetrate the micro-air gap and contradict the theory of lotus leaves. Therefore, scientists introduced the rose petal effect to explain the high adhesion of water molecules on the surface and the acquired WCA values (42). The rose petal effect showed that the micro-gap between the water droplet and the film's surface (theory of lotus leaf effect) was not observed due to high adhesion between the water and the TPCS films (43). The high WCA of the rose petal effect was due to the nano-gap structure surrounding the micro-roughness, which was responsible for the high WCA observed in TPCS/4B1C films. The AFM surface morphology of the TPCS/4B1C is shown in Figure 3b in a 3D topology form. The 3D topology indicates that the average roughness of the film's surface was 203.34 nm, proving that a nano-sized gap could be formed on the film's surface even though the TPCS films have a high affinity toward water molecules. The high nanoscale roughness surface is stipulated due to the homogenous agglomeration of nano-sized nanocellulose covered by the TPCS matrix, which formed a high roughness continuous network on the film's surface required for hydrophobicity. The high crystallinity of nanocellulose has a lower interaction with water molecules, which induces the nano-sized air gap within the microstructure. Meanwhile, for the TPCS/2B3C film, the random and inhomogeneous distribution of the hybrid nanofillers and porous structure on the film surface observed with an SEM caused an insufficient continuous, homogenous nano-sized roughness network structure to support the hydrophobic theory, thus leading to lower WCA.

3.4 WVP of TPCS, TPCS-SB, and TPCS-HB films

The significant disadvantages of the TPCS films are that high water sensitivity results in high water absorption and penetration through the films. The high water sensitivity properties of the TPCS films have provided the best environment for bacteria or microorganisms to grow inside the films. These may be beneficial for the biodegradability of the films; however, the rapid degradation of films will cause detrimental effects on the physical properties of films and reduce the film's service life. The water permeability properties of the TPCS films depend on the solubility coefficient and the water diffusion rate through the matrix. Incorporating a high crystallinity nanofiller or a layered structure filler could lower the moisture permeability by forming a more tortuosity pathway and hinder the water molecules from passing through the films.

Based on the results summarized in Table 2, the pure TPCS film exhibits the highest water permeability compared to all the films. The high water permeability increased drastically as the storage time increased. The drastic increase in water permeability was due to the high swelling properties of the TPCS matrix as a higher amount of water interacted with the TPS chain and plasticizer. The swelling of the TPCS matrix increases the size of the water passage and diffuses a higher amount of water through the films. The TPCS/5B film shows lower water permeability than the pure TPCS film across the storage time. The addition of bentonite clay decreases the water sensitivity of the TPCS film, and this is in line with many research studies as the clay layered structure was proved to be the most common method to reduce the water absorption in the polymer composite films. Even though the nanoclay addition was proved to be an effective way to reduce the water permeability of biopolymers, the toughness, clarity, and flexibility of the films were severely compromised as these three factors are the crucial properties for films packaging by creating a more prolonged and tortuous pathway in the film's matrix (44). Furthermore, good dispersion of the nanoclay layered structure in the matrix is critical in reducing the films' water permeability.

For the TPCS/5C film, the water weight loss was slow at the beginning of the storage period. However, the water weight loss rate increased drastically as the storage time increased. The low water permeability of the film may be attributed to the horrification effect of the nanocellulose during drying, causing the agglomeration of nanocellulose in the TPCS matrix and enhancement in the crystalline structure of the TPCS films. As the film ages, the effect of nanocellulose on resisting the water penetrating the film seemed to reduce. This may be due to water absorption into the microvoid between the interfacial nanocellulose/nanocellulose or nanocellulose/TPCS chains, causing the water molecules to diffuse into the films. The detachment of nanocellulose from the TPCS matrix led to the formation of a micro-crack close to the nanocellulose and induced higher water passing through the matrix. Besides, the high number of hydroxyl groups in the nanocellulose caused higher plasticizer to be surrounded within nanocellulose and the interfacial between nanocellulose and TPCS chain, and this also explains the sudden increase of water permeability of the TPCS/5C films. The distribution of glycerol in the matrix and the environmental humidity could affect the mass transport properties of the films. At the beginning of the storage, fewer water molecules were built up on the surface of the films, and glycerol could act as the filler to fill up the microvoid between nanocellulose and the TPCS matrix. Therefore, even though glycerol has a greater affinity toward nanocellulose, the water permeability resistance of the TPCS/5C was almost the same as TPCS/5B.

As the water permeation continued, the water molecules were built up from single water molecules layer to multiple water molecules layers and corresponded to the transition of a water adsorption mode to a water capillary diffusion mode into the matrix. Owing to the high hydrophilic property of glycerol, it possessed a higher affinity toward the water, thus more water molecules penetrated the films (45). The interaction of glycerol with water molecules could expand the gaps between the fibril and matrix and promote the TPCS chain's mobility and swelling to accommodate the passage of water molecules (46). Nevertheless, glycerol trapping around the interfacial space of nanocellulose and the TPCS chains caused different performances of TPCS/5C and TPCS/5B after the extended testing time.

The water permeability properties of the TPCS/nanocellulose biocomposite films might not always agree with each other in the literature due to different biocomposite compositions, surrounding humidity, processing method, testing, and accuracy of data collection. Some researchers reported that the high number of hydroxyl groups in the nanocellulose could induce higher water absorption into the films and weaken the intermolecular hydrogen bonding, facilitating the penetration of water molecules (19,20). The different outcomes of the water permeability properties of the TPCS/nanocellulose biocomposite may be attributed to the different orientations and distribution of nanocellulose in the films. On the other hand, some studies reported that the high crystallinity of nanocellulose could provide a water-repellent effect to the films in which fewer water molecules could interact with nanocellulose due to its high crystalline structure.

Apparently, TPCS/4B1C and TPCS/2B3C films showed a very low water permeability throughout the storage time, which does not correlate with the typical TPCS water permeability isotherms where the water permeability increased with the increase of storage time or RH. The low water permeability can be ascribed to nanocellulose, and the nanobentonite layered structure arranged parallel and alternatively to the surface of the TPCS, creating a double tortuosity pathway for the water molecules to pass through the films. As observed from Figure 4, the agglomeration of nanobentonite and nanocellulose was spotted in the TPCS/5B and TPCS/5C films, respectively. The non-uniform distribution of the single nanofiller in the TPCS matrix caused more “empty nanofiller spaces” compared to the biocomposite with hybrid nanofiller. Meanwhile, in the TPCS/HB, the distribution of the hybrid nanofillers was more homogenous compared to the TPCS/SB, resulting in a more restricted water pathway and lower water permeability.

The TPCS/4B1C has relatively lower water permeability than the TPCS/2B3C, which could be attributed to the smaller and good distribution of nanocellulose dispersed in the TPCS matrix. The excellent distribution of nanocellulose forms a high cohesive density with the TPCS matrix, reducing water molecules’ diffusion through the matrix. The bentonite nanoclay structure could counterbalance the hydrophilic properties of nanocellulose by protecting the nanocellulose from interacting with water when water molecules were adsorbed on the surface of the films. Figure 4d shows that the TPCS/4B1C contains a highly exfoliated nanoclay structure with well-distributed nanocellulose between the clay structures. The alternating structure of the nanobentonite/nanocellulose hybrid nanofillers in the TPCS/4B1C has effectively prevented water diffusion through the films. However, the resistance for water diffusion through the TPCS/HB films was compromised as the ratio of nanocellulose increased (2B3C) due to the inhomogeneous distribution of the hybrid nanofillers as observed in Figure 4e.

It is interesting to note that some researchers observed that even at a low amount of nanocellulose, the film’s water permeability was significantly reduced. The explanation was

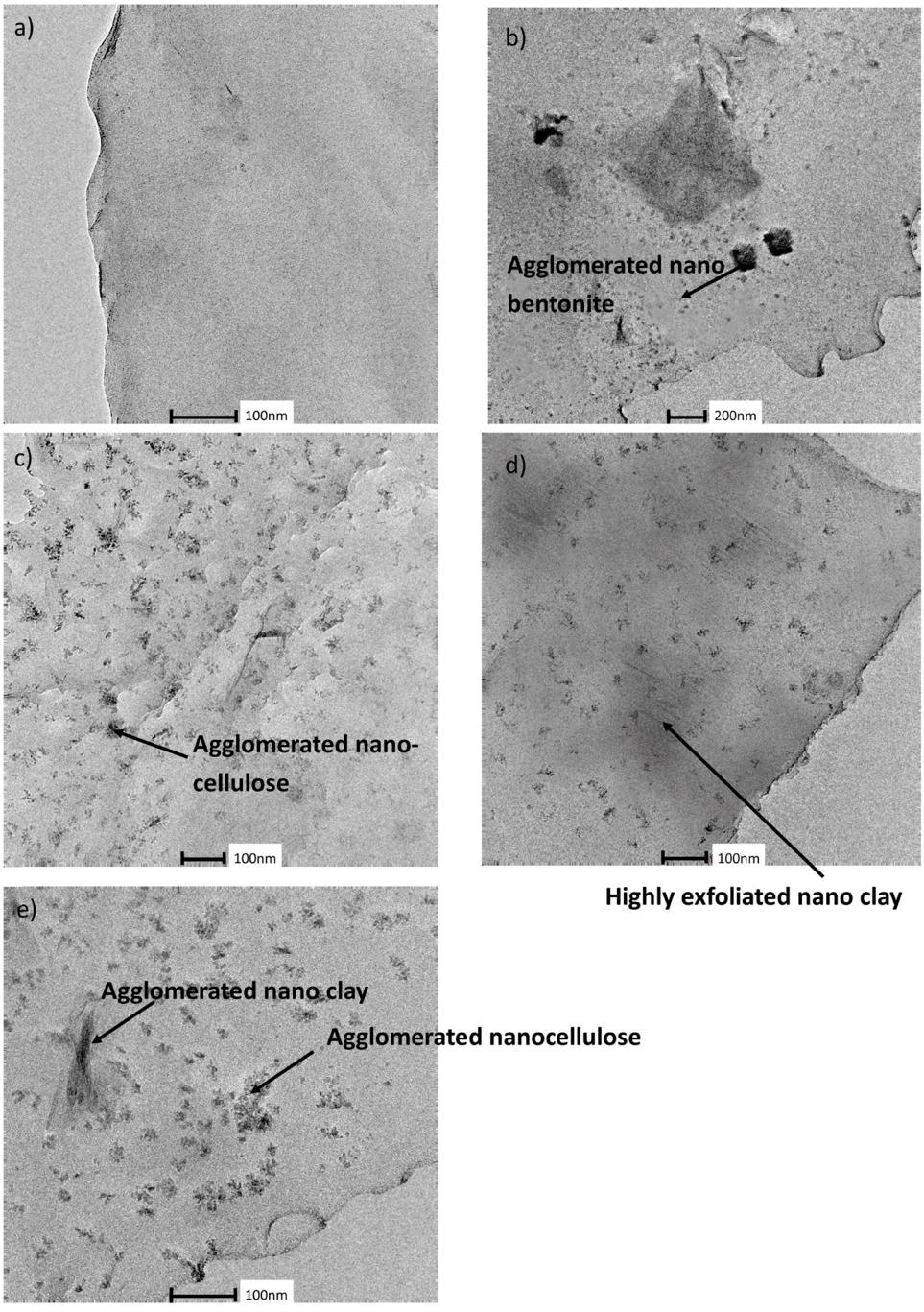

Figure 4: The TEM images of (a) TPCS, (b) TPCS/5B, (c) TPCS/5C, (d) TPCS/4B1C, and (e) TPCS/2B3C under magnification of 73,000×.

found in the review of Wang et al., where the high compatibility of nanocellulose with a matrix through hydrogen bonding can help to reduce the void, cracks, and other defects in the matrix and increase the crystallinity of the films to enhance the barrier properties of films (47). However, the inhomogeneous dispersion of the hybrid nanofiller in TPCS/2B3C resulted in a less perfect alternating tortuosity pathway in the matrix and allowed more water molecules to pass through the films.

3.5 Soil biodegradability of TPCS, TPCS-SB, and TPCS-HB films

It is essential to understand the biodegradability of films to assess the environmental impact of the films in the soils and help in better establishing policies to manage film waste under the legislation. Under an aerobic environment, fully biodegradable films will eventually transform entirely into carbon dioxide and water without

leaving any toxic by-products. The biodegradation of polymer always refers to the hydrolysis of ester bonds and the breaking down of the enormous polymer structure into monomers with the help of extracellular enzymes excreted by microorganisms. Glycoside hydrolases mainly degrade TPS and catalyze the glycosidic bonds' hydrolysis.

Before the degradation process, all the films exhibited transparent and smooth surface films; the surface of the films changed during the soil degradation period. All the films went through the same degradable phase with different duration of time. This biodegradable test identified three apparent biodegradable phases to categorize the TPCS films' biodegradability rate (48). The first stage is observed with a minimal weight loss of films (5–7% loss of the total film weight), where the biodegradable rate is the lowest as the bacterial or fungi only grow on the surface of the films. The films' integrity remained, and yellowish spots on the TPCS films were observed. For the second stage, the rapid loss of the weight of the films (60–70% loss of the total film weight) was observed with the fastest biodegradable rate. The high biodegradable rate was due to bacterial penetration into the matrix structure and biodegradation process across all the films. The film became brownish and highly brittle at this stage as microorganisms break down the basic matrix structure. The TPCS films act as biological fuel by providing glucose to support the growth of the microorganism. Apparent alterations to the film's appearance, such as pores, cracks, and crevices, were highly observed in the films. When reaching the last stage, the weight loss could not be calculated as the films were too brittle, broke into fractions, and were not easily removed from the soil. TPCS films become entirely the components in the soil, which can be used as a nutrient for other bacteria or plants to complete the carbon cycle.

In this study, all the films showed integrity in shape for up to 2 weeks (stage 1). However, after 2 weeks, the pure TPCS film was observed to be somewhat brittle and showed cracks in the structure. In week 3, the pure TPCS film was highly covered in the soil, and changes in the film's color were observed until the films were degraded entirely into a tiny fraction. The pure TPCS film took almost 1.5 months for the completion of the biodegradation process. The pure TPCS films showed a 70% loss in weight within 30 days (Figure 5), and the slow weight loss was observed in the starting first 14 days as the bacteria and fungi were only cultivated to grow surrounding the films. As the number of bacteria and fungi started to grow to an optimal amount, the biodegradation of the films became rapid, and a significant loss of mass of the films was observed. For the pure TPCS film, the

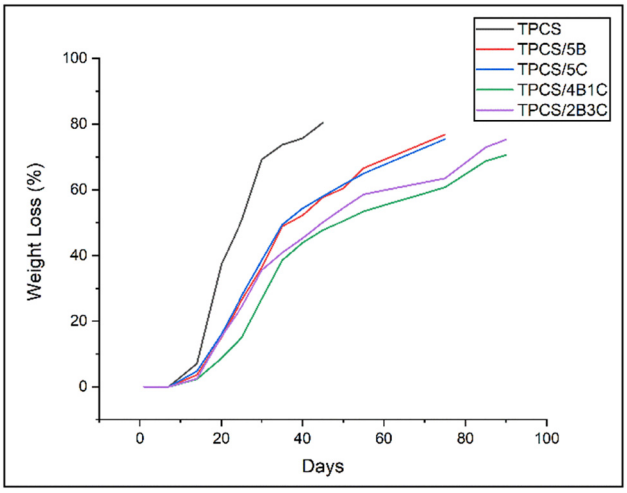

Figure 5: Weight loss (%) of TPCS, TPCS-SB, and TPCS-HB films.

transformation from phase 1 to phase 3 was relatively fast due to the high swelling of the TPCS matrix compared to other films. The high swelling property increased the matrix's volume, allowing higher water molecules to transfer into the films and promoting a sustainable environment for the film's microorganism growth (49).

Incorporating a nanofiller into the TPCS matrix was seen to prolong the stage 1 degradation process and reduced the TPCS biodegradable rate. Meanwhile, the soil degradation of TPCS-SB films was reduced as the film mass dropped significantly, and the change in the film color was only observed in week 4 (stage 2). On the other hand, the TPCS-HB films exhibited a significant mass drop and a change in the film's appearances in week 5. However, the TPCS-SB films have a higher degradation rate than the TPCS-HB film as the former only needs 90 days to fully degrade in the soil, while the TPCS-HB film requires almost 130 days for the completion of the degradation process. The prolonged biodegradation process showed that the hybrid nanofiller has effectively hindered the growth of the microorganism in the TPCS matrix by protecting the TPCS chains in the films. The lower water permeability and water solubility from the previous discussion suggest that the low penetration rate of water molecules into the films can be the main reason to explain the lowest biodegradable rate of this hybrid biocomposite system.

Comparing the biodegradable rate of the TPCS-SB films, TPCS/5B exhibited almost the same biodegradable rate as the TPCS/5C, even though nanocellulose showed higher hydrophilic properties than the bentonite in the biocomposite. The high biodegradable rate of the TPCS/5B films could be due to high porosity on the film's surface and high agglomeration of bentonite, which create a weak interfacial interaction between the bentonite and TPCS chains.

The weak interfacial interaction could lead to microvoids, facilitate the accumulation of water molecules in the TPCS matrix, and help bacterial growth. The TPCS-HB films degraded more slowly than the TPCS-SB films due to the lower water solubility, water absorption, and the highly compact TPCS matrix structure.

Previous studies showed that a significant fraction of the TPCS films would degrade into a small starch fraction or 80% loss in the mass in the soil within 1.5 months (50). In the review of Parsons et al., the average degradation rate of the TPCS biocomposite films can be varied between 7 and 18 weeks depending on the composition and the biodegradable ambient conditions (51). Even though the TPCS-HB films have a lower biodegradation rate than the TPCS-SB films and the pure TPCS film, the biodegradation rate of this material is still acceptable and appropriate for a biodegradable plastic (51,52). The lower biodegradation rate also proved the high stability of the TPCS-HB films under humidity and bacterial conditions, which is beneficial to expand the applicability of the films. The TPCS-HB films can be easily disposed of on the ground without leaving any toxic residual in the soil, reducing the environmental problem and the costs of waste management procedures.

Li et al. found that the molecular and crystalline structure of starch could affect the enzymatic degradation of the TPCS films, where the fast degradation occurs at the amorphous and small TPCS chains region located at the film surface (53). This could be due to the high susceptibility of the amorphous region to be attacked by fungi or bacteria. Meanwhile, the high crystalline structure in the TPCS matrix could reduce the film's degradation rate due to the highly compact structure, which limits the penetration of water molecules and microbial growth. Therefore, by observing the progress of the film's degradation process, the films' crystalline and amorphous regions could be roughly estimated as the degradation of films always starts at the amorphous region.

For the first 14 days, all the films maintained their integrity, and a slight weight alteration was observed. The weight of the pure TPCS films shows a slight increase due to water absorption from the soils. Meanwhile, the weight of other films remained relatively stable for the first 14 days. After 14 days, all the films started to turn brownish due to the adhered soil on the film's surface and the microorganisms' growth, as shown in Figure 6. However, for the pure TPCS film, the physical characteristics of the film started changing from flexible to brittle, and the film was broken down into two pieces, showing that microorganisms can easily penetrate the TPCS matrix and hydrolyze the structure into two components. The pure TPCS films have the least resistance to microorganisms, where the biodegradation of the films has moved into phase 2 much earlier than other films. Meanwhile, TPCS-SB films (TPCS/5B and TPCS/5C films) only showed the first appearance of cracks or holes in the structure after the first 30 days. On the contrary, the TPCS/4B1C and TPCS/2B3C films showed only minor degradation marks on the films after the first 50 days.

Certainly, the film surface morphology observed in Figure 2 could be related to the films' physical transformation and biodegradation rate during the soil degradation. The high film's porosity could lead to higher water accumulation in the pores, creating an optimal environmental condition for micro-bacterial growth and subsequently accelerating the biodegradation process (54). Pure TPCS has the highest biodegradation rate, and thus, severe film erosion can be observed with the highest pore surface density. As a single nanofiller (nanocellulose or nanobentonite) was incorporated, the pores formed on the film's surface were observed to be reduced, and the biodegradation rate and physical erosion of the films became slower compared to the pure TPCS. Meanwhile, TPCS/4B1C and TPCS/2B3C films were observed to have the lowest physical erosion, and the film's integrity remained after 50 days. The delayed film's physical erosion is attributed to the highly compact film's surface, which prevents microbacterial growth in the deeper layers of the film and retards the penetration of microbacteria.

As all the films entered their phase 2 biodegradation, they exhibited a high rate of weight loss according to their respective biodegradation rate. All the films eventually entered phase 3 and became highly fractional in the soil. One interesting observation can be concluded from the film's degradation morphology, where different macroscopic changes are detectable by observing their physical biodegradation image; perhaps, they could be related to the filler dispersion in the films. The microorganisms grow in the films and are "fed on" the films. The propagation of the micrometric path or the creation of a hole in the films could be used as the indicator for the pathway of the microorganism highly located and growing (55). Therefore, the surface and structural degradation can be used to locate nanofillers' dispersion, as nanofillers could slow down the growth of the microorganism in the films.

For the TPCS/5C film, the localized biodegradation region was spotted at the bottom of the films, as shown in Figure 6. For the TPCS/5B film, biodegradation was observed at the upper and lower parts of the film. As time progressed, there was a significant propagation of crack and fractionalization across the TPCS/5B film.

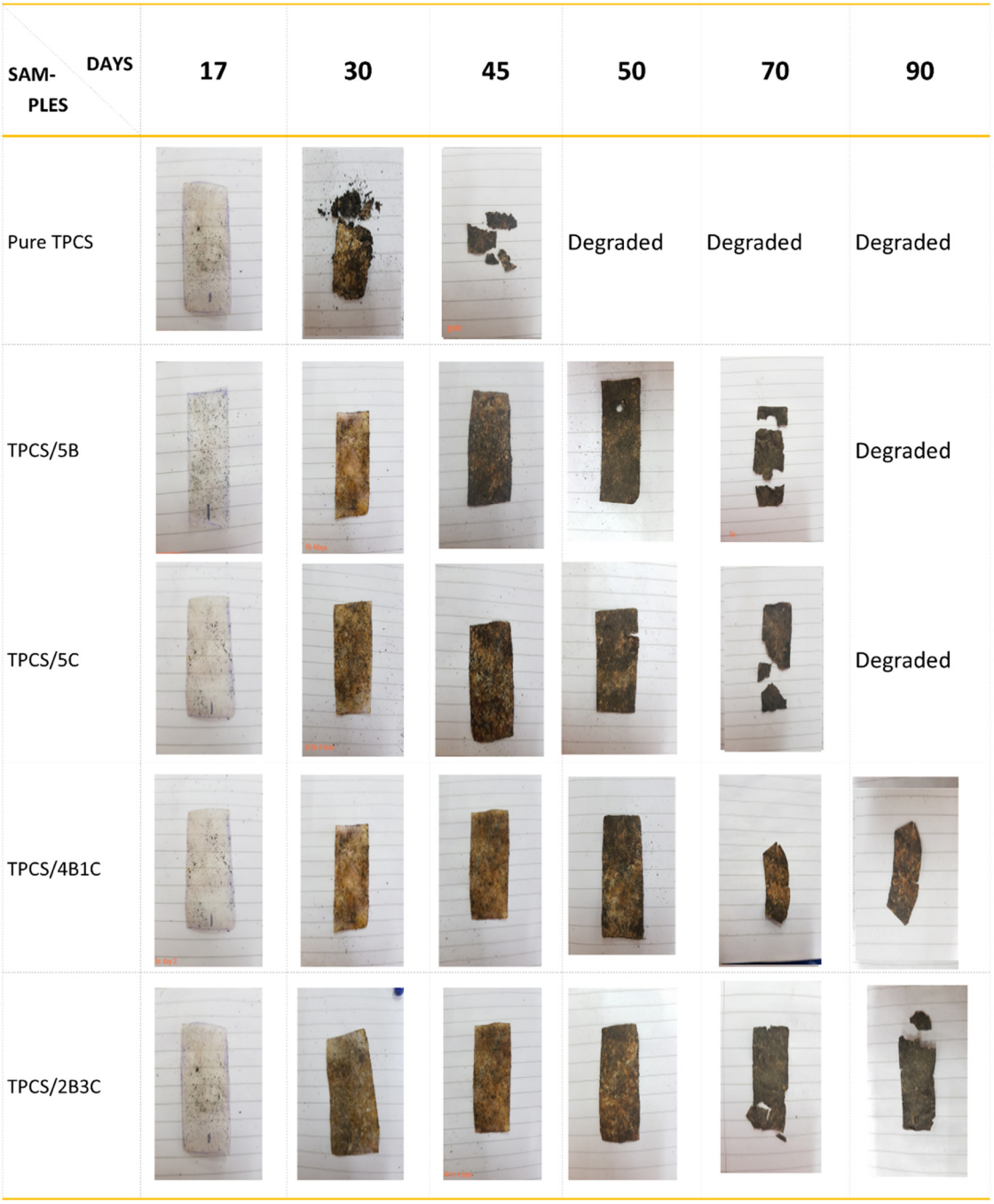

Figure 6: Physical transformation of pure TPCS, TPCS-SB, and TPCS-HB films in 3 months during soil biodegradation.

Meanwhile, the TPCS/5C exhibited much slower film degradation than the TPCS/5B, and fractionalization mainly occurred at the bottom of the films. The different morphologies of crack propagation and fractionalization behaviors of both films could be related to a better dispersion of nanocellulose and lower pore density in the TPCS/5C compared to the TPCS/5B, which provided higher protection to the TPCS chains and reduced the growth of the microorganisms in the films.

In contrast, the biodegradation of the TPCS/4B1C film started at the film's edge and the crack propagated slowly, moving from the edge toward the middle of the film. The biodegradation only occurred along the edge of the films, suggesting that the microorganisms unfavorably grow on the film surface due to the high compact nacre structure and low water permeability, which hinder the microorganism growth within the film's matrix.

Generally, the TPCS/2B3C film shows almost an identical biodegradable spot with the TPCS/4B1C film; however, due to the inhomogeneous dispersion of the hybrid nanofillers, the microorganisms got more chance to grow and prompt a crack across the film, thus breaking the film into two pieces.

4 Conclusions

The hydration characteristics and biodegradability of the TPCS, TPCS-SB, and TPCS-HB were analyzed via water absorption, water solubility, WCA, water permeability, and soil biodegradability. Based on the reported results, the TPCS-HB films exhibit a significant improvement in water resistance properties than the TPCS and TPCS-SB films. The surface of the TPCS-HB film was observed to be highly compact, with fewer pores and a higher degree of WCA, which was attributed to the lower absorption of water on the surface. Meanwhile, the synergistic interactions of the hybrid filler nanobentonite and nanocellulose in the TPCS matrix were proved to be more effective than the single nanofiller in preventing the penetration of water molecules through the films. The TPCS/4B1C exhibits the best water resistance properties and the lowest rate of soil biodegradability. This indicates that the optimal water resistance properties of the TPCS-HB films could be achieved by adjusting the ratio of the hybrid nanofiller to 4:1 (nanobentonite and nanocellulose, respectively). The low water sensitivity and water permeability of the TPCS/4B1C have greatly enhanced the film's stability as the water diffusion through the film was significantly reduced. The improved film's stability and water resistance properties of the TPCS/4B1C indicate its promising potential as a biodegradable packaging material. With these features, it can be applied to pack dried and semi-dried products, as a single-use bioplastic.

Funding information: The authors gratefully acknowledge the funding and the financial support from the Fundamental Research Grant Scheme (FRGS) – (FRGS/1/2019/TK10/UNIMAP/03/2) funded by the Ministry of Higher Education Malaysia.

Author contributions: Azlin Fazlina Osman, Andrei Victor Sandu: conceptualization, investigation, methodology, writing – review, and editing; Sinar Arzuria Adnan: conceptualization and project administration; Di Sheng Lai, Shayfull Zamree Abd Rahim: data curation, formal analysis, investigation, methodology, and writing – original draft; Ismail Ibrahim, Petrica Vizureanu: project administration, visualization, and methodology.

Conflict of interest: The authors state no conflict of interest.

Data availability statement: The data presented in this study are available on request from the corresponding author.

References

(1) Surendren A, Mohanty AK, Liu Q, Misra M. A review of biodegradable thermoplastic starches, their blends and composites: Recent developments and opportunities for single-use plastic packaging alternatives. Green Chem. 2022;24:8606–36.
(2) Csiszar E, Kun D, Fekete E. The role of structure and interactions in thermoplastic starch-nanocellulose composites. Polymers (Basel). 2021;13(18):3186.
(3) Cheng H, Chen L, McClements DJ, Yang T, Zhang Z, Ren F, et al. Starch-based biodegradable packaging materials: A review of their preparation, characterization and diverse applications in the food industry. Trends Food Sci Technol. 2021;114:70–82.
(4) Bangar SP, Whiteside WS. Nano-cellulose reinforced starch biocomposite films-A review on green composites. Int J Biol Macromol. 2021;185:849–60.
(5) Akaishi A, Yonemaru T, Nakamura J. Formation of water layers on graphene surfaces. ACS Omega. 2017;2:2184–90.
(6) Huang S, Chao C, Yu J, Copeland L, Wang S. New insight into starch retrogradation: The effect of short-range molecular order in gelatinized starch. Food Hydrocoll. 2021;120:106921.
(7) Tabasum S, Younas M, Zaeem MA, Majeed I, Majeed M, Noreen A, et al. A review on blending of corn starch with natural and synthetic polymers, and inorganic nanoparticles with mathematical modeling. Int J Biol Macromol. 2019;122:969–96.
(8) Wu H, Lei Y, Lu J, Zhu R, Xiao D, Jiao C, et al. Effect of citric acid induced crosslinking on the structure and properties of potato starch/chitosan composite films. Food Hydrocoll. 2019;97:105208.
(9) Paluch M, Ostrowska J, Tyński P, Sadurski W, Konkol M. Structural and thermal properties of starch plasticized with glycerol/urea mixture. J Polym Environ. 2021;30:728–40.
(10) Osman AF, Ashafee AMTL, Adnan SA, Alakrach A. Influence of hybrid cellulose/bentonite fillers on structure, ambient, and low temperature tensile properties of thermoplastic starch composites. Polym Eng Sci. 2020;60:810–22.
(11) Adnan SA, Ranjamdin AN, Osman AF, Ibrahim I, Sheng LD, Zaidi NHA, et al. Mechanical properties of thermoplastic starch/oil palm empty fruit bunch biocomposite film. Proceedings of Green Design and Manufacture 2020. Arau, Malaysia: AIP Publishing LLC; 2021.
(12) Brand W, van Kesteren PC, Swart E, Oomen AG. Overview of potential adverse health effects of oral exposure to nanocellulose. Nanotoxicology. 2022;16(2):1–30.

(13) Brandelli A. Toxicity and safety evaluation of nanoclays. In: Mahendra Rai JKB, editor. Nanomaterials: ecotoxicity, safety, and public perception. Switzerland: Springer; 2018. p. 57–76.
(14) Henning FG, Ito VC, Demiate IM, Lacerda LG. Non-conventional starches for biodegradable films: A review focussing on characterisation and recent applications in food. Carbohydr Polym Technol Appl. 2021;4:100157.
(15) Lambert S, Wagner M. Environmental performance of bio-based and biodegradable plastics: the road ahead. Chem Soc Rev. 2017;46:6855–71.
(16) Rivadeneira-Velasco KE, Utreras-Silva CA, Díaz-Barrios A, Sommer-Márquez AE, Tafur JP, Michell RM. Green nanocomposites based on thermoplastic starch: A review. Polymers. 2021;13:3227.
(17) Kargarzadeh H, Huang J, Lin N, Ahmad I, Mariano M, Dufresne A, et al. Recent developments in nanocellulose-based biodegradable polymers, thermoplastic polymers, and porous nanocomposites. Prog Polym Sci. 2018;87:197–227.
(18) Derungs I, Rico M, López J, Barral L, Montero B, Bouza R. Influence of the hydrophilicity of montmorillonite on structure and properties of thermoplastic wheat starch/montmorillonite bionanocomposites. Polym Adv Technol. 2021;32:4479–89.
(19) Syafri E, Yulianti E, Asrofi M, Abral H, Sapuan S, Ilyas R, et al. Effect of sonication time on the thermal stability, moisture absorption, and biodegradation of water hyacinth (Eichhornia crassipes) nanocellulose-filled bengkuang (Pachyrhizus erosus) starch biocomposites. J Mater Res Technol. 2019;8:6223–31.
(20) Asrofi M, Abral H, Putra YK, Sapuan S, Kim H-J. Effect of duration of sonication during gelatinization on properties of tapioca starch water hyacinth fiber biocomposite. Int J Biol Macromol. 2018;108:167–76.
(21) Wei Z, Sinko R, Keten S, Luijten E. Effect of surface modification on water adsorption and interfacial mechanics of cellulose nanocrystals. ACS Appl Mater Interfaces. 2018;10:8349–58.
(22) Lourenço AF, Gamelas JA, Nunes T, Amaral J, Mutjé P, Ferreira PJ. Influence of TEMPO-oxidised cellulose nanofibrils on the properties of filler-containing papers. Cellulose. 2017;24:349–62.
(23) Zhang K, Ismail MY, Liimatainen H. Water-resistant nanopaper with tunable water barrier and mechanical properties from assembled complexes of oppositely charged cellulosic nanomaterials. Food Hydrocoll. 2021;120:106983.
(24) Ramesh P, Prasad BD, Narayana K. Influence of montmorillonite clay content on thermal, mechanical, water absorption and biodegradability properties of treated kenaf fiber/PLA-hybrid biocomposites. Silicon. 2021;13:109–18.
(25) Mansour G, Zoumaki M, Marinopoulou A, Tzetzis D, Prevezanos M, Raphaelides SN. Characterization and properties of non-granular thermoplastic starch—Clay biocomposite films. Carbohydr Polym. 2020;245:116629.
(26) Kwaśniewska A, Chocyk D, Gładyszewski G, Borc J, Świetlicki M, Gładyszewska B. The influence of kaolin clay on the mechanical properties and structure of thermoplastic starch films. Polymers. 2020;12:73.
(27) Islam H, Susan M, Imran AB. Effects of plasticizers and clays on the physical, chemical, mechanical, thermal, and morphological properties of potato starch-based nanocomposite films. ACS Omega. 2020;5:17543–52.
(28) Wu C-N, Saito T, Fujisawa S, Fukuzumi H, Isogai A. Ultrastrong and high gas-barrier nanocellulose/clay-layered composites. Biomacromolecules. 2012;13:1927–32.
(29) Garusinghe UM, Varanasi S, Raghuwanshi VS, Garnier G, Batchelor W. Nanocellulose-montmorillonite composites of low water vapour permeability. Colloids Surf A Physicochem Eng Asp. 2018;540:233–41.
(30) Lai DS, Osman AF, Adnan SA, Ibrahim I, Alrashdi AA, Ahmad Salimi MN, et al. On the use of OPEFB-derived microcrystalline cellulose and nano-bentonite for development of thermoplastic starch hybrid bio-composites with improved performance. J Polym. 2021;13:897.
(31) Lai DS, Osman AF, Adnan SA, Ibrahim I, Ahmad Salimi MN, Alrashdi AA. Effective aging inhibition of the thermoplastic corn starch films through the use of green hybrid filler. Polymers. 2022;14:2567.
(32) Blahovec J, Yanniotis S. GAB generalized equation for sorption phenomena. Food Bioprocess Technol. 2008;1:82–90.
(33) Boinovich L, Emelyanenko A. A wetting experiment as a tool to study the physicochemical processes accompanying the contact of hydrophobic and superhydrophobic materials with aqueous media. Adv Colloid Interface Sci. 2012;179:133–41.
(34) Aguirre-Loredo RY, Rodriguez-Hernandez AI, Velazquez G. Modelling the effect of temperature on the water sorption isotherms of chitosan films. Food Sci Technol. 2016;37:112–8.
(35) Kulasinski K, Guyer R, Keten S, Derome D, Carmeliet J. Impact of moisture adsorption on structure and physical properties of amorphous biopolymers. Macromolecules. 2015;48:2793–800.
(36) Rajabnezhad S, Ghafourian T, Rajabi-Siahboomi A, Missaghi S, Naderi M, Salvage JP, et al. Investigation of water vapour sorption mechanism of starch-based pharmaceutical excipients. Carbohydr Polym. 2020;238:116208.
(37) Asay DB, Kim SH. Evolution of the adsorbed water layer structure on silicon oxide at room temperature. J Phys Chem B. 2005;109:16760–3.
(38) He Y, Tang H, Chen Y, Zhang S. Facile strategy to construct metal–organic coordination thermoplastic starch with high hydrophobicity, glass-transition temperature, and improved shape recovery. ACS Sustain Chem Eng. 2020;8:8655–63.
(39) Yin P, Chen C, Ma H, Gan H, Guo B, Li P. Surface cross-linked thermoplastic starch with different UV wavelengths: mechanical, wettability, hygroscopic and degradation properties. RSC Adv. 2020;10:44815–23.
(40) Gutiérrez TJ, Ollier R, Alvarez VA. Surface properties of thermoplastic starch materials reinforced with natural fillers. Funct Biopolym. 2018;131–58.
(41) Bhushan B, Nosonovsky M. The rose petal effect and the modes of superhydrophobicity. Philos Trans R Soc A Math Phys Eng Sci. 2010;368:4713–28.
(42) Milionis A, Ruffilli R, Bayer IS. Superhydrophobic nanocomposites from biodegradable thermoplastic starch composites (Mater-Bi®), hydrophobic nano-silica and lycopodium spores. RSC Adv. 2014;4:34395–404.
(43) Wang F, Qiu L, Tian Y. Super anti-wetting colorimetric starch-based film modified with poly (dimethylsiloxane) and micro-/nano-starch for aquatic-product freshness monitoring. Biomacromolecules. 2021;22:3769–79.
(44) Enescu D, Frache A, Geobaldo F. Formation and oxygen diffusion barrier properties of fish gelatin/natural sodium

montmorillonite clay self-assembled multilayers onto the biopolyester surface. RSC Adv. 2015;5:61465–80.
(45) Faradilla R, Lee G, Roberts J, Martens P, Stenzel M, Arcot J. Effect of glycerol, nanoclay and graphene oxide on physicochemical properties of biodegradable nanocellulose plastic sourced from banana pseudo-stem. Cellulose. 2018;25:399–416.
(46) Minelli M, Baschetti MG, Doghieri F, Ankerfors M, Lindström T, Siró I, et al. Investigation of mass transport properties of microfibrillated cellulose (MFC) films. J Membr Sci. 2010;358:67–75.
(47) Wang J, Gardner DJ, Stark NM, Bousfield DW, Tajvidi M, Cai Z. Moisture and oxygen barrier properties of cellulose nanomaterial-based films. ACS Sustain Chem Eng. 2017;6:49–70.
(48) Zain AHM, Ab Wahab MK, Ismail H. Biodegradation behaviour of thermoplastic starch: the roles of carboxylic acids on cassava starch. J Polym Environ. 2018;26:691–700.
(49) Oz H, Aris A, Levi A, Uluagac AS. A survey on ransomware: Evolution, taxonomy, and defense solutions. ACM Comput Surv. 2022;54:1–37.
(50) Bulatović VO, Grgić DK, Slouf M, Ostafinska A, Dybal J, Jozinović A. Biodegradability of blends based on aliphatic polyester and thermoplastic starch. Chem Pap. 2019;73:1121–34.
(51) Polman EMN, Gruter GM, Parsons JR, Tietema A. Comparison of the aerobic biodegradation of biopolymers and the corresponding bioplastics: A review. Sci Total Env. 2020;753:141953.
(52) Kjeldsen A, Price M, Lilley C, Guzniczak E, Archer I. A review of standards for biodegradable plastics. Ind Biotechnol Innov Cent. 2018;33:13–6.
(53) Li M, Witt T, Xie F, Warren FJ, Halley PJ, Gilbert RG. Biodegradation of starch films: The roles of molecular and crystalline structure. Carbohydr Polym. 2015;122:115–22.
(54) Ruggero F, Carretti E, Gori R, Lotti T, Lubello C. Monitoring of degradation of starch-based biopolymer film under different composting conditions, using TGA, FTIR and SEM analysis. Chemosphere. 2020;246:125770.
(55) Corrêa AC, de Campos A, Claro PIC, Guimarães GGF, Mattoso LHC, Marconcini JM. Biodegradability and nutrients release of thermoplastic starch and poly (ε-caprolactone) blends for agricultural uses. Carbohydr Polym. 2022;282:119058.